Numerical modelling of resolution and sensitivity of ERT in horizontal boreholes

Danielsen, Berit Ensted; Dahlin, Torleif

Published in:
Journal of Applied Geophysics

DOI:
10.1016/j.jappgeo.2010.01.005

2010

Link to publication

Citation for published version (APA):
Danielsen, B. E., & Dahlin, T. (2010). Numerical modelling of resolution and sensitivity of ERT in horizontal boreholes. *Journal of Applied Geophysics*, *70*(3), 245-254. https://doi.org/10.1016/j.jappgeo.2010.01.005

Total number of authors:
2

General rights
Unless other specific re-use rights are stated the following general rights apply:
Copyright and moral rights for the publications made accessible in the public portal are retained by the authors and/or other copyright owners and it is a condition of accessing publications that users recognise and abide by the legal requirements associated with these rights.
• Users may download and print one copy of any publication from the public portal for the purpose of private study or research.
• You may not further distribute the material or use it for any profit-making activity or commercial gain
• You may freely distribute the URL identifying the publication in the public portal

Read more about Creative commons licenses: https://creativecommons.org/licenses/

Take down policy
If you believe that this document breaches copyright please contact us providing details, and we will remove access to the work immediately and investigate your claim.

LUND UNIVERSITY

PO Box 117
221 00 Lund
+46 46-222 00 00

Download date: 26. Jun. 2024

Author's personal copy

Journal of Applied Geophysics 70 (2010) 245–254

Contents lists available at ScienceDirect

Journal of Applied Geophysics

journal homepage: www.elsevier.com/locate/jappgeo

Numerical modelling of resolution and sensitivity of ERT in horizontal boreholes

Berit E. Danielsen *, Torleif Dahlin

Engineering Geology, Lund University, Box 118, 221 00 Lund, Sweden

ARTICLE INFO

Article history:
Received 6 August 2007
Accepted 20 January 2010

Keywords:
ERT
Horizontal boreholes
Numerical modelling
Arrays
2D sensitivity patterns
Non-parallel
Water filled boreholes

ABSTRACT

Resistivity in horizontal boreholes can give useful detailed information about the geological conditions for construction in rock, i.e. in front of a tunnel bore machine. This paper is an attempt to identify a suitable methodology for an effective measuring routine for this type of geophysical measurements under actual construction site conditions.

Prior to any measurements numerical modelling was done in order to evaluate the resolution of different electrode arrays. Four different arrays were tested; dipole–pole, cross-hole dipole–dipole, cross-hole pole–tripole and multiple gradient array. Additionally the resolution of a combination of cross-hole dipole–dipole and multiple gradient was assessed. The 2D sensitivity patterns for various arrangements of the cross-hole dipole–dipole and multiple gradient array were examined. The sensitivity towards inaccurate borehole geometry and the influence of water in the boreholes were also investigated. Based on the model study the cross-hole dipole–dipole array, multiple gradient array and a combination of these were found to give the best result and therefore were used for test measurements in horizontal boreholes. The boreholes were 28.5 m long and drilled 6.5 m apart. Prototypes of semi-rigid borehole cables made it possible to insert multi electrode cables in an efficient way, allowing fast measurement routines. These measurements were then studied to determine their accuracy and applicability. The results showed a high resistivity rock mass at the site. A transition from high resistivity to slightly lower resistivity coincides well with a change in lithology from gneiss-granite to gneiss. It is likely that the shotcrete on the tunnel wall is seen as a low resistivity zone. The measurements are a valuable tool, but further development of the cables and streamlining of measuring routines have to be performed before the resistivity tomography can be used routinely in pilot holes during construction in rocks.

© 2010 Elsevier B.V. All rights reserved.

1. Introduction

Pre-investigations are vital for time efficient, cost efficient and safe construction in rock. This requires sufficient knowledge about the rock properties such as water flow and stability. During tunnel drilling with a tunnel boring machine (TBM) probe drillings are made in front of the TBM on a regular basis. If the geology varies on a small scale, then probe drillings might not be representative of the rock mass between the boreholes. Thus the aim with this study is to investigate the possibility of using these boreholes for electrical resistivity tomography (ERT). ERT can be done between two or more boreholes and gives information about the rock mass between the boreholes. An important task is to make the whole measuring routine fast and efficient in order to avoid any delay for the TBM.

At geotechnical site investigations electrical imaging in combination with core drilling and geophysical logging has proven to be valuable for providing information about rock quality and detailed information on the engineering geological characteristics (Dahlin et al., 1999). Rønning (2003) investigated the usefulness of surface based geophysical methods in the early stages of construction work. The conclusion is that 2D resistivity investigations often can indicate a weak zone, but this depends on the contrast between the resistivity of the weak zone and the surrounding rock. Electrical imaging made from the surface gives limited resolution at greater depths, and for more detailed information borehole measurements are required.

Previously ERT in vertical boreholes has proven useful for environmental investigations (Daily et al., 1995; Daily and Owen, 1991; Deceuster et al., 2006; French et al., 2002; Goes and Meekes, 2004; Guérin, 2005; LaBrecque et al., 1996). The method has also been demonstrated as economically efficient in wells drilled during geotechnical pre-investigation of a tunnelling site to obtain a 2D image of the resistivity close to a TBM (Denis et al., 2002). Here the method could detect vertical and horizontal changes in the soil. It thereby gave information about the geology between the wells. The measurements were done from the surface in sedimentary rocks while the measurements in this study are performed at tunnel level and in crystalline rock.

Even though model studies investigating the resolution of different electrode arrays have been done previously (Bing and Greenhalgh, 2000; Danielsen et al., 2005; Goes and Meekes, 2004) it was found necessary to perform a new study focussing on the specific scenario at

* Corresponding author. Engineering Geology, Lund University, Sweden.
E-mail address: berit.danielsen@tg.lth.se (B.E. Danielsen).

0926-9851/$ – see front matter © 2010 Elsevier B.V. All rights reserved.
doi:10.1016/j.jappgeo.2010.01.005

Author's personal copy

the tunnel site. The influence of water in the boreholes is investigated for a 3D model which is inverted as 2D. For a 2D case the model recovery of different electrode arrays is investigated in order to find the best suited array for the particular geology. The 2D sensitivity patterns for various arrangements of the cross-hole dipole–dipole and multiple gradient array are examined in order to clarify the modelling results.

Wilkinson et al. (2008) investigated the effects of geometric errors on cross-hole resistivity using analytical methods. In our case the importance of the geometry of the probe drillings was investigated through numerical modelling. The geometry of the boreholes is in reality very uncertain because they are drilled without precision. Therefore it is not known how parallel the holes actually are. What is interesting and relevant is to observe the magnitude of the error in data when data is inverted assuming that the boreholes are parallel. 3D inversion is possible, but given the data acquisition, it is not of relevance here.

This paper describes first the numerical modelling carried out to test how different electrode arrays recover structures in a specific geological setting. It is also investigated how uncertainty in the borehole geometry and water in the boreholes influences the results. For the numerical modelling the borehole separation and the electrode distance are equal to the actual measurements. Then the results from the numerical modelling are shown and discussed before the measurement using ERT in horizontal boreholes are presented. The measurements were carried out on an experimental stage. The first measurements were made in a tunnel where problems with poor rock quality have delayed the work seriously. The boreholes used were similar to those drilled as probe drillings in front of the TBM. They were 28.5 m long and drilled 6.5 m apart, with a diameter of 64 mm. The results from the measurements are discussed before the conclusions from the modelling and the test measurements are given.

2. Numerical modelling

This section is divided into two parts. The first part comprises the setup of the numerical study and the second part describes the results. In the numerical study the model recovery and the sensitivity of different array types towards uncertainty in the geometry of the boreholes are assessed. Before the main modelling is done the influence of low resistive water in the boreholes is investigated. The essence with the modelling is to represent and test realistic field setup, inversion software and geological scenarios for this specific case.

In all cases two 19.5 m long boreholes separated with 6.5 m are modelled. The models resemble crystalline rock with high resistivity. In the first model there is an inclined low resistive feature e.g. water-bearing fracture zones. In the second model there is an inclined zone with a slightly lower resistivity than the matrix resembling a different lithology. The resistivity contrast is much lower than in the first model. The air-filled tunnel front is considered as having a very high resistivity.

The forward modelling is done in RES2DMOD (Loke, 2002) using a finite difference grid. The model is 50 m by 130 m (see Fig. 1). The grid size is 0.25 m by 0.25 m in the part of the model where the boreholes

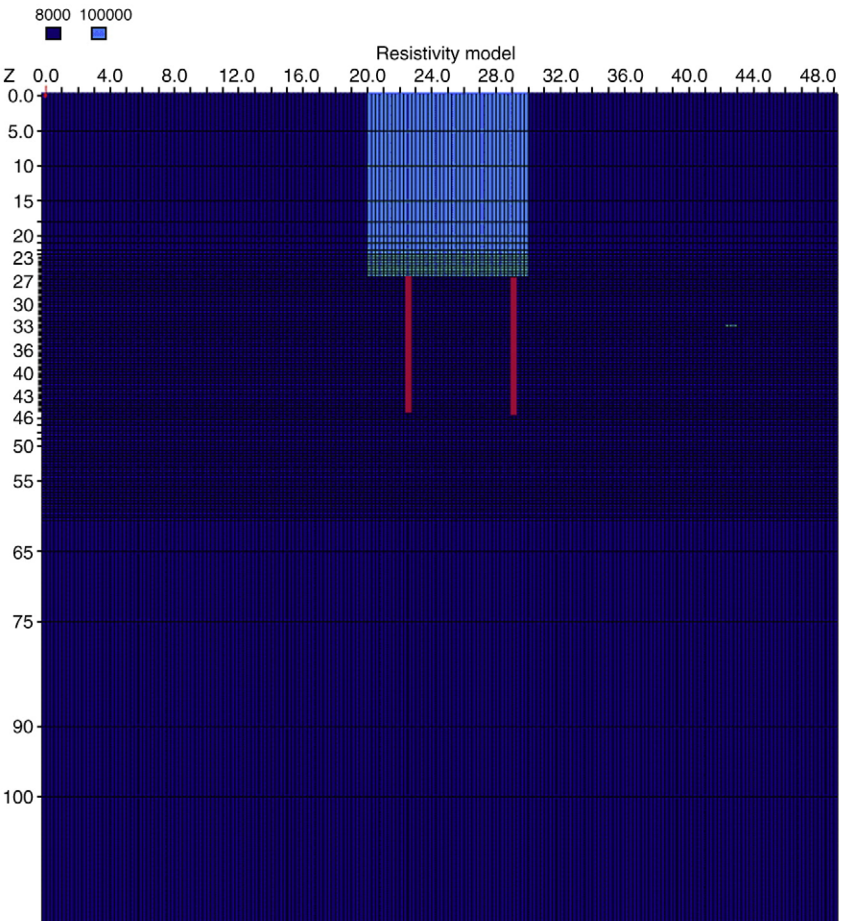

Fig. 1. The full model showing the boundaries. The red lines are the position of the boreholes. The grid size is 0.25 times 0.25 m in the section where the boreholes are positioned.

Author's personal copy

are. The boreholes are positioned at 22.5 m and 29 m and the electrodes are positioned from 26 to 45 m with 0.5 m spacing. Only the area of the models where there is sensitivity towards the geology is shown in the examples. Prior to inversion 5% random noise was added to the apparent resistivity data.

The inversion is done in RES2DINV (Loke, 2004a,b) with a robust inversion (L_1-norm), by which the sum of the absolute values of the data misfit is minimized. The robust inversion was chosen because of the relatively sharp boundaries and large contrast in the resistivity (Loke et al., 2003). The residual between the forward calculated resistivities and the model response is used to verify the quality of the inversion, which in the case of robust inversion is calculated as the mean of the absolute values of the differences between the input data and the model response data, i.e. (Claerbout and Muir, 1973):

$$residual = mean((\underline{d}^{\,obs} - \underline{d}\,))$$

where $\underline{d}^{obs}$ is a vector containing the measured data and $\underline{d}$ is the vector of the forward response calculated from the model (pseudo-section). Multiplication with 100% gives the residual in percent. It is expected that the residual is in the same magnitude as the random noise added to the apparent resistivity, provided the inversion has been successful in finding a model in agreement with the data.

Four electrode arrays were tested (see Fig. 2); dipole–pole (AM-N), cross-hole dipole–dipole (AM-BN), cross-hole pole–tripole (A-BMN) (Goes and Meekes, 2004) and multiple gradient (Dahlin and Zhou, 2004). Then different combinations of gradient, AM-BN and A-BMN were tested but only the combination of AM-BN and multiple gradient is shown here. This is done because those two gave the best result when they were used alone. The dipole–pole (AM-N) and cross-hole dipole–dipole (AM-BN) are popular arrays in which Bing and Greenhalgh (2000) gave good results for environments where the resistivity contrast is a factor 10. In Goes and Meekes (2004) the pole–tripole (A-BMN) gave good results for tests done in unconsolidated sediments. In our case the arrays are tested for larger resistivity contrast in crystalline bedrock. The multiple gradient configuration has not previously been tested for borehole measurements. This is a surface array which here is converted to a borehole array and is a combination of two single-hole datasets. The surface gradient array is addressed further in Dahlin and Zhou (2004). The number of data points (Table 1) influences the time used for measuring and inversion of the data. Because the time used for performing the measurements and the inversion are very important when used in front of a TBM the datasets are as small as possible. Both the gradient and the AM-BN have a relatively limited number of data points when implemented in the way done in our tests, i.e. with one s-factor for the gradient array and limited maximum separation between the dipoles.

The dipole–dipole configuration AB-MN was also tested at an initial stage but without satisfactory results, as was the case in the study by Bing and Greenhalgh (2000). Bing and Greenhalgh (2000) showed that the cross-hole pole–dipole A-MN, dipole–pole AB-M and the dipole–dipole AB-MN have singularity problem in data acquisition, giving many near-to-zero potential values. Therefore these alternatives are not considered here.

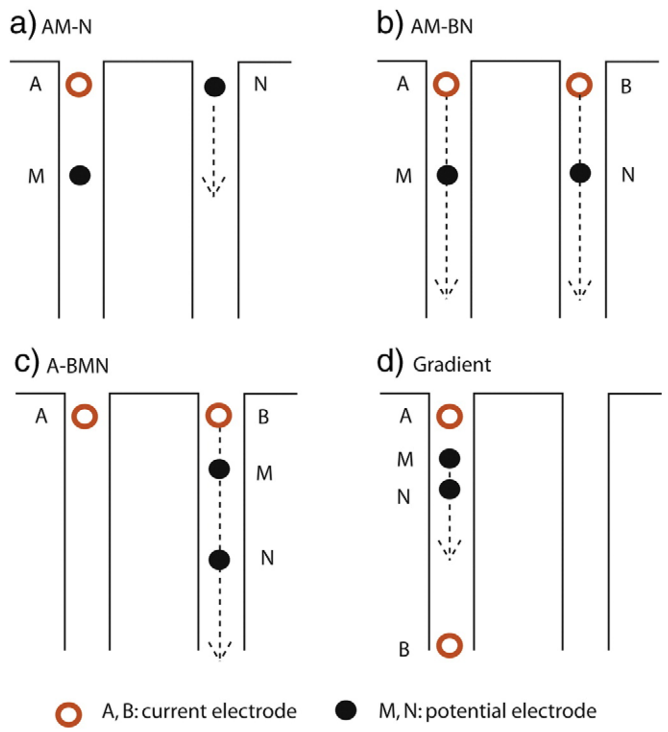

Fig. 2. Schematic layout of the discussed electrode configurations.

2.1. Resolution of different electrode arrays

Before the resolution of different electrode arrays is assessed the influence of water in the boreholes is roughly evaluated. During actual measurements water is present in the boreholes. The risk is that the water in the boreholes is so conductive that the current never will enter the bedrock but only pass through the water.

In reality the measurements are 3D but in this case only 2D inversion of the data are considered. Thus the forward modelling is made with RES3DMOD (Loke, 2001) and afterwards the data are extracted as 2D data and inverted in RES2DINV. Since finite difference is used (rectangular grid) the boreholes have to be approximated as having square cross section. The grid size is still 0.25 m by 0.25 m, but because the borehole is situated in a grid node, the boreholes have to be modelled as 0.5 m by 0.5 m even though the actual diameter of the boreholes is 0.06 m. The calculations are based on the equivalence principals i.e. the ratio between the layer thickness and the resistivity has to be constant, e.g. Parasnis (1986); Reynolds (1997). To obtain a correct *total conductance* of the grid cells representing the boreholes, the resistivity has to be approximately 100 times larger than in the actual case. The resistivity of the water in some wells at the investigation area is measured to be 50 Ω m on average. Therefore the resistivity of the boreholes in the model should be 5000 Ω m. This means that the contrast between the boreholes and matrix is very small and consequently the water in the boreholes is expected to be unimportant. To be on the safe side the modelling was carried out using a resistivity of 500 Ω m (i.e. the actual water resistivity is 5 Ω m) and a resistivity of 8000 Ω m for the matrix. If water in the borehole is critical for the measurements the very low resistivity would definitely influence the model recovery.

In Fig. 3 the 2D inversion of the 3D model shows that the very low resistivity of the boreholes is not recovered. For all four arrays the resistivity of the area between the boreholes is higher than in the forward model. One extremity is the AM-BN in Fig. 3c where the resistivity close to the boreholes is the same as for the forward modelling matrix. The other extremity is the gradient array (Fig. 3e)

Table 1
Number of data points in four different electrode arrays and the combined array used in this numerical modelling. The arrays are generated using Matlab.

Array	Number of data points for 2D
Dipole–pole (AM-N)	640
Dipole–dipole (AM-BN)	268
Pole–tripole (A-BMN)	720
Gradient	248
Gradient + AM-BN	516

Author's personal copy

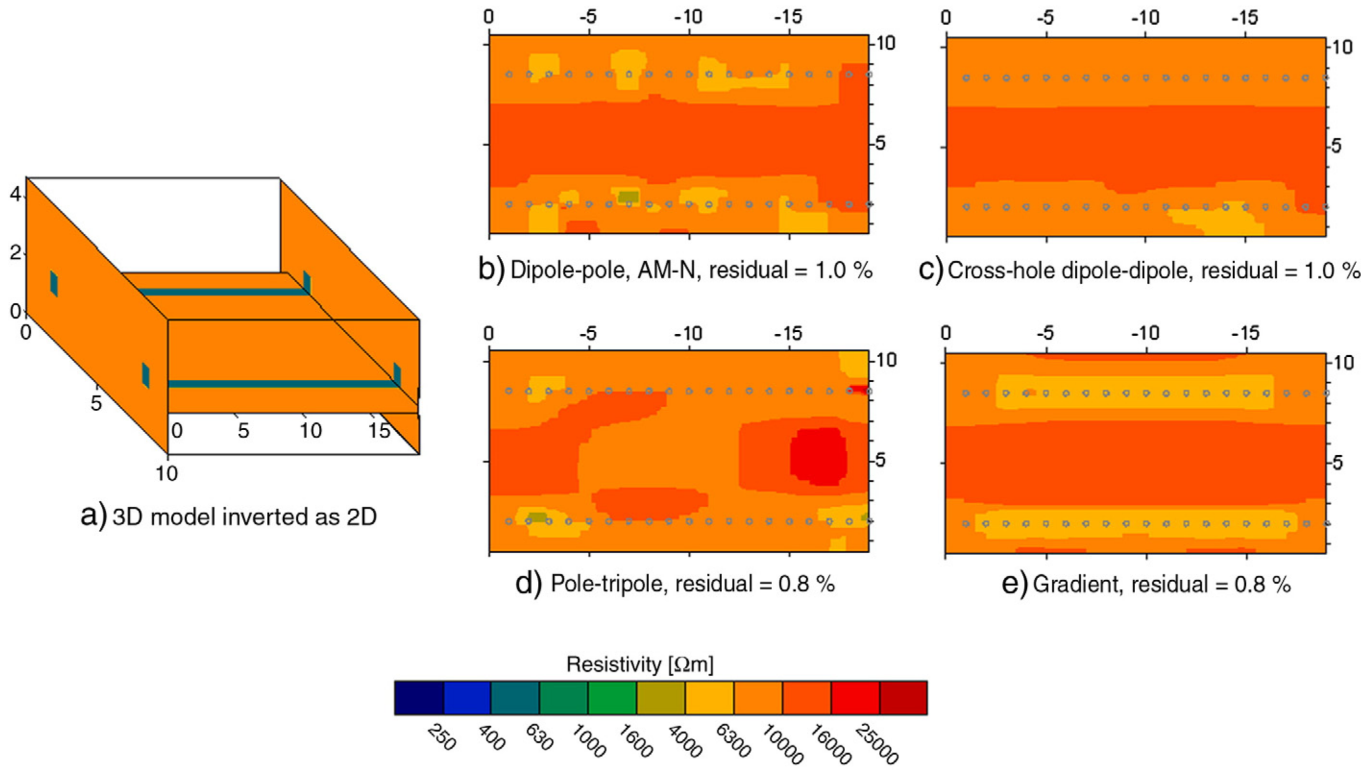

Fig. 3. a) The 3D model is inverted as 2D. The matrix has a resistivity of 8000 Ω m and the borehole has a resistivity of 500 Ω m. Inversion results using b) dipole–pole (AM-N), c) cross-hole dipole–dipole(AM-BN), d) pole–tripole (A-BMN), e) multiple gradient. The distance is in metre.

where the resistivity close to the boreholes is lower than the matrix, but not as low as the true borehole resistivity. In between is the AM-N and A-BMN where there are some areas with lower resistivity and some with higher. But for none of the arrays the recovery of the matrix resistivity is influenced by the very low resistivity of the boreholes. Therefore the boreholes are assumed to be of minor importance with regards to the resistivity results and are excluded from the further study of the model recovery.

The first model used for the study of the model recovery has an inclined fracture zone with a resistivity of 300 Ω m in an 8000 Ω m matrix, see Fig. 4a. The high resistivity area in the left side of the model is the air-filled tunnel front. In the second model there is a wide inclined zone with a slightly lower resistivity (3000 Ω m) compared to the matrix (8000 Ω m). This resembles the contrast between two lithologies such as gneiss and gneiss-granite. Such a contrast is what can be expected in the field measurements.

The electrode arrays have a 0.5 m electrode spacing, thus there are 40 electrodes in each borehole. The total number of electrodes is larger than the maximum possible in the forward modelling program RES2DMOD. Therefore the generation of data is done twice with 1 m electrode spacing, where the second is displaced by 0.5 m compared to the first.

2.2. Sensitivity towards borehole geometry

The sensitivity towards the geometry of the boreholes is very important to assess because the probe drillings in front of a TBM are not drilled with great precision. In the worst case the accuracy is in the order of 1–2 m on a 40 m long borehole. It is too expensive and time consuming to measure the geometry of the boreholes. As a consequence the electrodes are most likely in different positions when the data are measured than the position assumed in the data inversion. This means that when performing the inversion some inaccurate assumptions are made because the electrode geometry will be imprecise.

For modelling this scenario model 1 is used as in the section on electrode array resolution, where the electrodes in the left borehole diverge increasingly from a straight line with depth as illustrated by the red dots in Fig. 7a. The modelling is done for smaller and larger distances between the boreholes. The results were similar, thus only the latter is shown here.

The left borehole deviates 1 m in 19 m. Data is generated with these two non-parallel boreholes, but when inverting data, parallel boreholes are assumed. For evaluating the result the inverted data are compared with the ideal situation where the boreholes are in fact parallel when generating the data. This comparison is made by calculating the relative change. The difference in resistivity between the normal and diverging dataset is divided by the resistivity of the diverging dataset.

2.3. Results of the numerical modelling

2.3.1. The ability to recover the models using different arrays

Modelling the ability of the different arrays to recover the models showed differences in their ability to resolve the resistivity and location of the geological features. The results from the inversion of the synthetic model are shown in Figs. 4 and 5. Figs. 4a and 5a show the true models created in RES2DMOD. The models are seen from above with a left (L) and right (R) borehole.

In Fig. 4b–e the results are shown where only one array type is used on model 1. For all four arrays the correct thickness and position of the low resistivity zone are resolved accurately only at the boreholes. Therefore the best resolution is close to the electrodes. Except for the A-BMN the arrays have a slightly higher resistivity in a large area at the tunnel front. Experiments with adding a priori information to the data before inversion, e.g. fixed region and known boundaries, did not improve the result. The model residual is 7% for the AM-N whereas it is 3.8% for both AM-BN and A-BMN and 2.3% for the gradient array. As expected the model residual is in the same magnitude as the added noise (5%). There are cases of fitting the

Author's personal copy

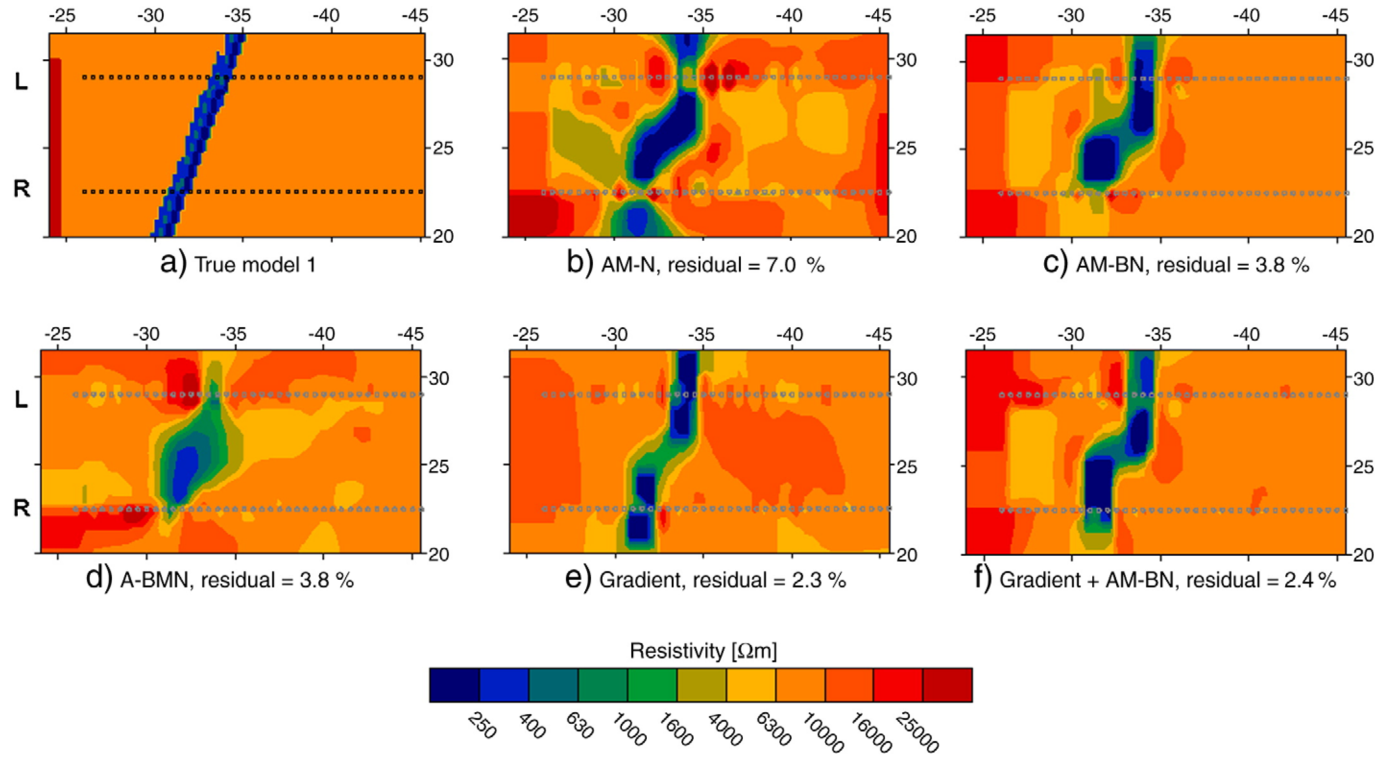

Fig. 4. a) The true model 1 made in RES2DMOD. Model of inclined fracture zone with a resistivity of 300 Ω m in a 8000 Ω m matrix. The model is seen from above with a left (L) and right (R) borehole. Inversion results using b) dipole–pole (AM-N), c) cross-hole dipole–dipole (AM-BN), d) pole–tripole (A-BMN), e) gradient, f) combination of gradient and cross-hole dipole–dipole. Black and grey dots are the electrodes in the boreholes. The distance is in metres.

model to the noise, which is seen as small islands (artefacts) of deviant resistivity at a single electrode, e.g. for the gradient array (Fig. 4e) at 27 m in the left borehole. This can also occur for field measurements but is easy to diagnose. The A-BMN in Fig. 4d has most difficulties in resolving the low resistivity zone. The zone is more diffuse and has a higher resistivity at the edges of the model than the AM-N, AM-BN and multiple gradient arrays (Fig. 4b, c and e). These three arrays resolve the resistivity of the inclined zone well. With AM-N the inclined zone is

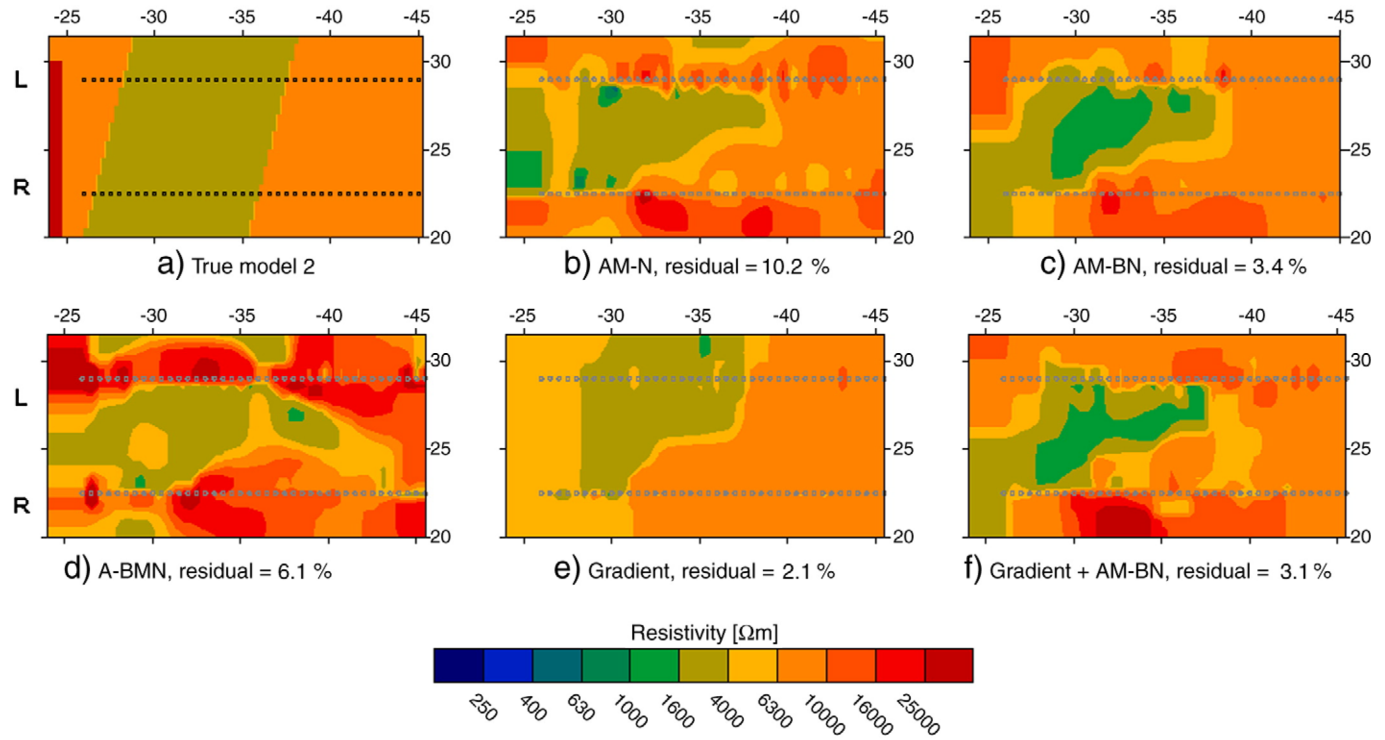

Fig. 5. a) The true model 2 made in RES2DMOD. Model of inclined zone with a resistivity of 3000 Ω m in a 8000 Ω m matrix. The model is seen from above with a left (L) and right (R) borehole. Inversion results using b) dipole–pole (AM-N), c) cross-hole dipole–dipole (AM-BN), d) pole–tripole (A-BMN), e) gradient, f) combination of gradient and cross-hole dipole–dipole. Black and grey dots are the electrodes in the boreholes. The distance is in metres.

Author's personal copy

resolved as continuous and with a homogeneous resistivity. The matrix is not well resolved and there are several artefacts, where data are fitted to noise. The multiple gradient array can resolve both the matrix and the inclined layer and the transition between high and low resistivity is particularly narrow. For the AM-BN array the inclined zone is diffuse and too large. Close to the tunnel front the resistivity of the matrix is too low. There are a few artefacts but the array resolves the matrix well.

The combination of AM-BN and multiple gradient array is seen in Fig. 4f. This combination has a residual of 2.4% and therefore fits the data well. The low resistivity zone appears in steps but is close to having the true resistivity. The transition from high to low resistivity is narrow. As in the case for the AM-BN array, the resistivity close to the tunnel front is too low.

In Fig. 5b–e the results are shown where only one array type is used on model 2. It is seen that AM-N, A-BMN and gradient can recover the resistivity of the wide low resistive zone in the area between the boreholes. The residual for AM-N is 10.2% which is considerably higher than for the other arrays. The AM-BN in Fig. 5c underestimates the resistivity of the low resistive zone. However, the geometry of the zone is not recovered well, especially not at the edges of the model. The residual is 3.4% for the AM-BN indicating a good fit to the data. The AM-N and AM-BN in Fig. 5b and c are very similar in how the true model is recovered. At the boreholes there are high resistive circular areas located around one or two electrodes which are considered to be artefacts i.e. fitting model to noise. The resistivity of the matrix is well recovered. The A-BMN in Fig. 5d is dominated by high resistivity close to boreholes. The resistivity of the matrix is clearly overestimated. The residual is 6.1% which supports the visual impression of a poor data fit. The gradient array in Fig. 5e has no artefacts and recovers the resistivity and geometry of the different zones. It is only the area close to the tunnel front where the resistivity is slightly underestimated. For this array the residual is as low as 2.1% giving a good fit to the data.

In Fig. 5f the combination of gradient and AM-BN is shown. It is clear that the AM-BN dominates the result giving an underestimation of the low resistive zone and an overestimation of the resistivity in the bottom of the figure outside the right borehole. The residual is 3.1% which is a good data fit.

Fig. 6 shows the 2D sensitivity pattern for three AM-BN (a–c) and three gradient (d–f) electrode configurations. Other combinations were studied and these are some representative examples. Observe that the scale used for the AM-BN configurations is one magnitude larger than the scale used for the gradient configurations. It is quite clear that the AM-BN has a greater sensitivity between the boreholes. The sensitivity decreases quite rapidly when the separation between the current and potential electrodes increases. The gradient configuration has a smaller sensitivity between the boreholes, but has a much larger sensitivity close to the electrodes. Because of the different sensitivity patterns the arrays are expected to have different advantages in resolving geological structures, which the results in Figs. 4 and 5 show.

2.3.2. Sensitivity towards borehole geometry

Fig. 7 shows the results from modelling the sensitivity to different degrees of divergence from parallel. The figure show the relative change instead of the resistivity image since the difference in the resistivity image is small. A change between −0.25 and 0.25 (white) indicates zones that show almost no difference between the case when the boreholes are perfectly parallel and when they are not. The red colour

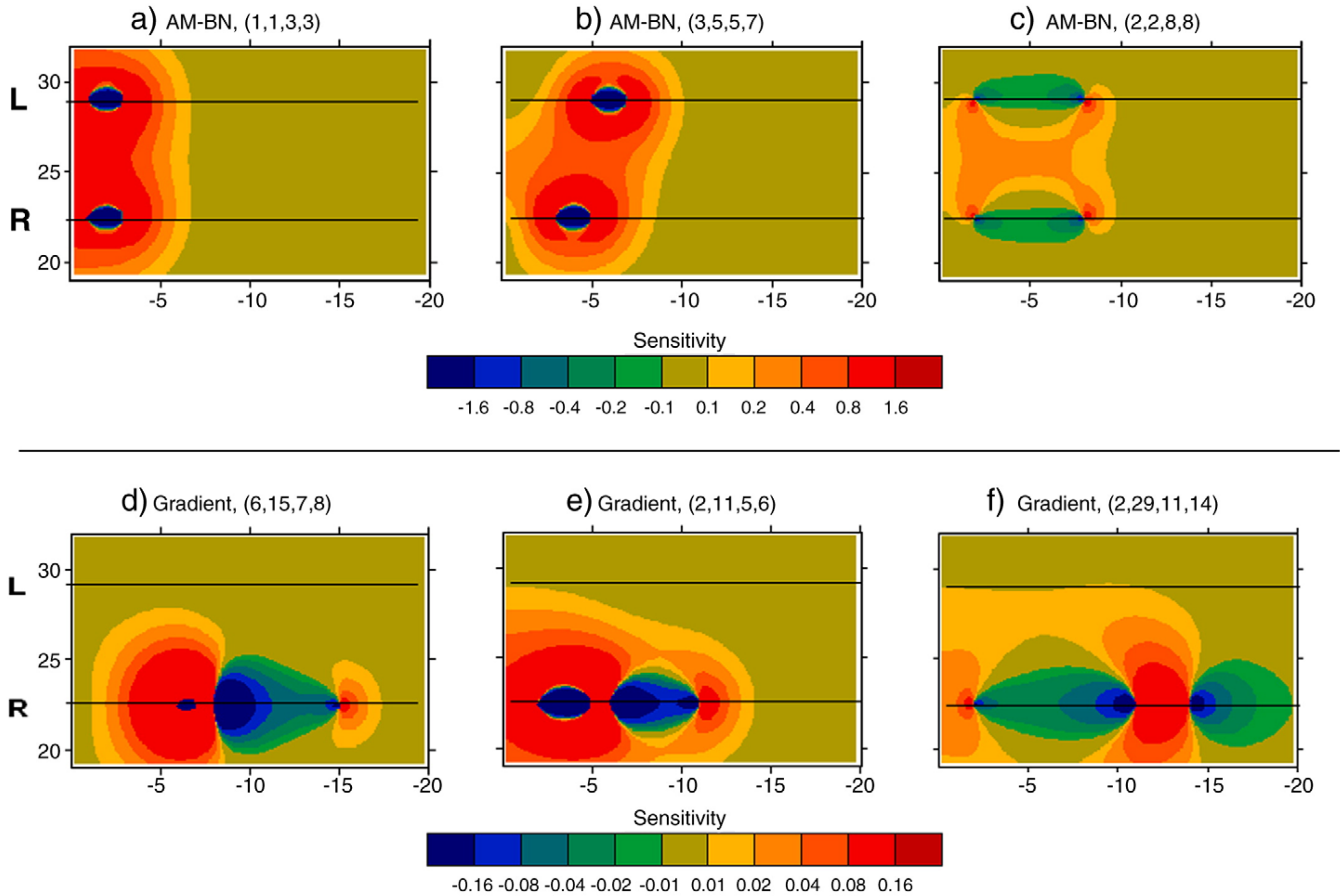

Fig. 6. The 2D sensitivity pattern in horizontal boreholes using AM-BN, a)–c), and multiple gradient, d)–f). The position of the electrodes (C1, C2, P1, and P2) is given in brackets. The horizontal black lines mark the position of the two boreholes. The distance is in metres. Notice the difference of a factor ten between the sensitivity of AM-BN and multiple gradient.

Author's personal copy

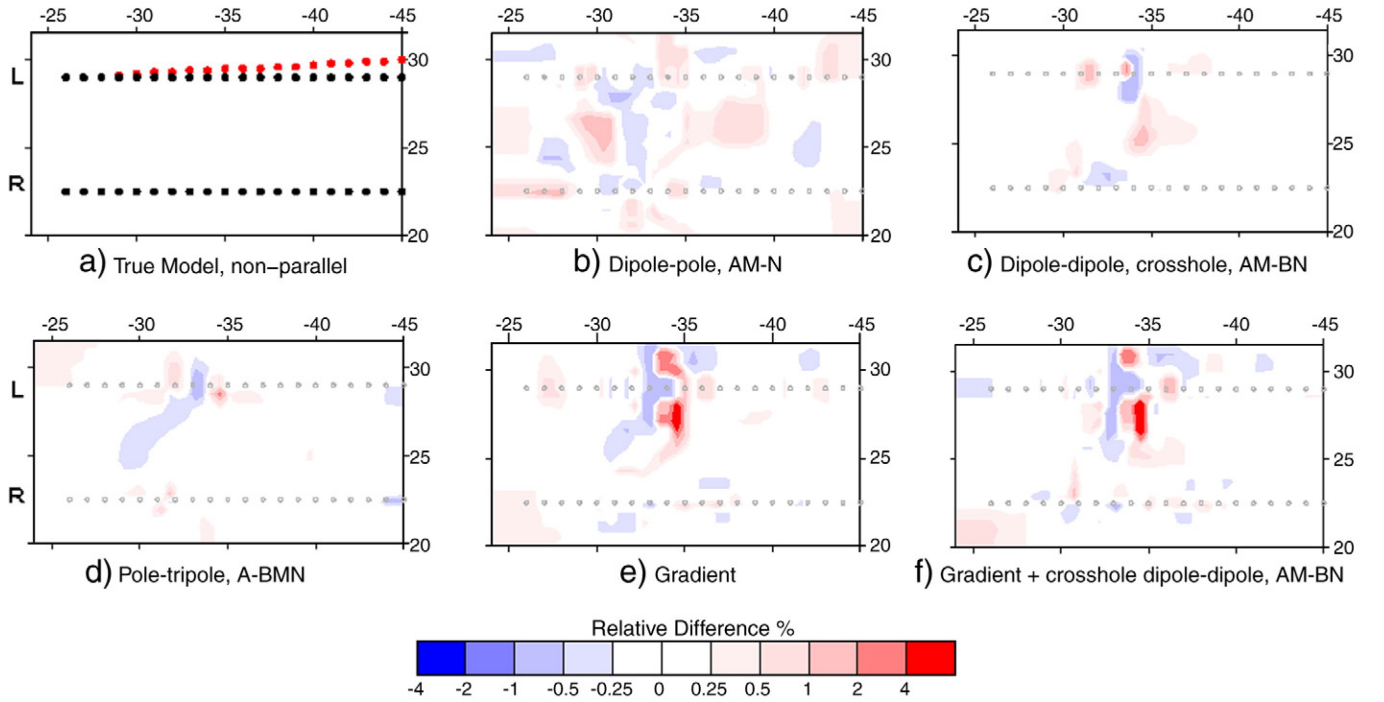

Fig. 7. The relative difference between inverted models with parallel and non-parallel boreholes. a) The red dots are the position of the electrodes while data are generated. The black dots are the position of the electrodes while the data are inverted. b) dipole–pole (AM-N), c) cross-hole dipole–dipole (AM-BN), d) pole–tripole (A-BMN), e) gradient, f) combination of gradient and cross-hole dipole–dipole (AM-BN). The grey dots are the electrodes in the boreholes assumed during inversion. The distance is in metres.

indicates that the resistivity obtained by the inclined borehole is smaller than for the parallel boreholes. The opposite is the case for the blue colour.

The AM-N array in Fig. 7b, is relatively sensitive towards changes in borehole geometry. The AM-BN array, Fig. 7c, and the A-BMN, Fig. 7d, are sensitive close to the low resistivity zone but are generally insensitive elsewhere. The largest difference is seen with the gradient array in Fig. 7e. At the low resistivity zone in the left borehole the relative difference is large. The combination of gradient and AM-BN sums up the differences from the individual arrays (Fig. 7f).

3. Discussion of the numerical modelling

Generally the numerical modelling showed that the area best recovered is close to the electrodes for all the arrays.

The best recovery of the resistivity and position of the geological structures is obtained with multiple gradient array, AM-BN and a combination of AM-BN and multiple gradient array. These arrays have the lowest residual (~2–6%). In all cases the matrix and the low resistivity close to the boreholes are well resolved. Even though the resistivity contrast in model 2 is small the arrays recover the model well. This is useful in the actual case where there is expected to be a difference in lithology and therefore a small difference in resistivity. The AM-BN is good at resolving the resistivity of the matrix between the boreholes but there are some artefacts. The study of the 2D sensitivity patterns for the AM-BN and gradient array supports these observations. The gradient array has a smaller sensitivity between the boreholes than the AM-BN. Results from other modelling carried out, but not shown here, emphasise that the resolution between and outside the boreholes is limited for the gradient array. This is probably due to the fact that it is two single-hole data sets merged together. It can be expected that it creates symmetry problems as described in Tsourlos et al. (2003). This has to be addressed further in the future. By combining the two arrays the structures are slightly better resolved. The AM-N has a high residual (7–10%). The array resolves the low resistivity zone, but not the matrix where there are quite a number of artefacts. The A-BMN has a relatively high residual for model 2. The configuration does not have the same resolution of this geological setting as AM-N, AM-BN and multiple gradient configurations.

The signal to noise ratio for the different arrays is important to consider when evaluating the results. The geometric factor is calculated for each electrode configuration because it is inversely proportional with the signal to noise ratio (Loke, 2004a,b). The geometrical factor for the A-BMN differs between 20 and 10,000 whereas AM-BN mainly differs between 10 and 1000. Even though A-BMN has some electrode configurations with high signal to noise ratio, there are also many configurations with low signal to noise ratio. The gradient array has a geometrical factor between 25 and 250 which is the lowest for the array tested. Therefore the gradient also has the highest signal to noise ratio. This influences the resolution of the models and contributes to the overall impression of the arrays' performance.

The study of the sensitivity of the arrays towards the borehole geometry showed that the smallest difference is obtained using the AM-BN or A-BMN. The sensitivity towards geometry errors was visualized by using the relative difference instead of the actual inversion model. This was done because the difference is difficult to distinguish when comparing the inversion models. This demonstrates that the geometry problem produces only small changes in the resistivity values. In most cases the difference is largest close to the low resistivity zone. A limitation in the study is that only one of the boreholes is deviates because it is not possible to model two inclined boreholes in RES2DMOD. In reality the geometry is probably that both boreholes are deviating. In such a case there will be a larger difference, but it is expected that for the array types discussed, this will produce only a minor difference.

With the particular application in mind, i.e. measurements in front of a TBM, it is very important that the measurements and inversion is fast. The measurements can only be performed when the TBM is

Author's personal copy

standing still and the information about the geology is needed before the production can be resumed. Therefore it is crucial with fast data acquisition and inversion, hence an approach that requires as few data points as possible without compromising resolution and reliability is desired. This is a critical factor because, as shown in e.g. Dahlin and Loke (1998), the data density is important for resolving certain structures. With the computer power available the data is inverted within 5 min, and with faster computers this reduces so it is of minor importance. The time used on the data acquisition depends on e.g. the instrument, number of stacks, measurement delays and integration time. These factors depend on the field conditions and can only be determined at the field site. A rough assessment for a 4 channel instrument and combination of gradient and AB-MN (Table 1) would give 129 measurements. Each measurement takes between 2 and 20 s, depending on selected parameters and site conditions, which means that the whole acquisition can take between 4 and 40 min. In addition there is a certain mobilization time for getting the cables ready for measuring. This rough estimation shows that several factors influence the time used on measurements. Still the optimization of the number of data points should be addressed further in future work.

Based on the results from the numerical modelling the AM-BN and the gradient arrays were used in the field test measurements in the horizontal boreholes. It is then possible to combine the different datasets before inversion. Even though Goes and Meekes (2004) showed good results for the A-BMN, it did not resolve the geology particularly well for the models studied and has a high residual. The A-BMN also had a low signal to noise ratio. Thus the A-BMN was not used for the actual measurements in the boreholes. The AM-N array did not prove to be good at resolving the matrix giving very high residual, and was also sensitive towards unknown borehole geometry. In addition the array is more complicated to use in the field, because of the need for a remote electrode.

4. ERT in horizontal boreholes

Horizontal boreholes raise several practical questions, i.e. how to get the electrode cables into the boreholes. For solving this problem a prototype of a semi-rigid cable has been developed, using a thin fibreglass rod to create rigidity, Fig. 8. A further requirement is that the cables can be wound up so that they can be handled in confined spaces. To avoid getting stuck in the boreholes the cables have to be streamlined. The need to have streamlined cables conflicts with the requirement for adequate electrode contact with the borehole walls. To overcome this both test holes were drilled with a couple of degrees inclination downwards in order to keep water in the holes thus creating better electrode contact. The inclination also makes it possible to pour water into the hole if no water is present naturally.

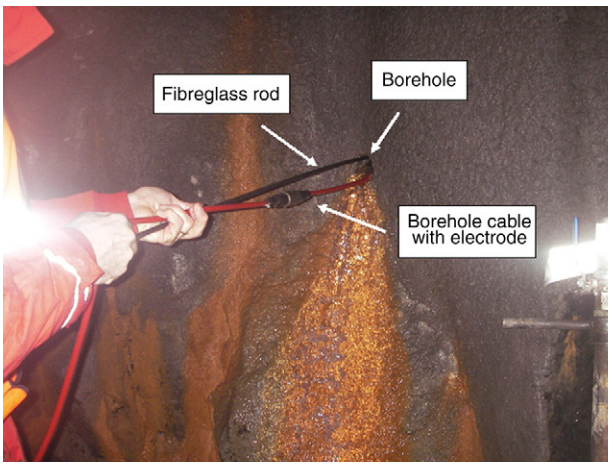

Fig. 8. Photograph of a borehole cable with the thin fibreglass rod.

For the test measurements the electrode spacing was 1 m, but by pulling back the electrode cable half a metre after the first measurement and then measuring a second time the data interval was reduced to 0.5 m. It should be noted, however, that any measurements with 0.5 m electrode spacing could not be done.

For the measurements the Lund Imaging system was used, in this case consisting of Terraohm RIP924, ABEM Electrode Selector ES10-64C and ABEM SAS2000 Booster. The same array protocols were used in field as in the numerical modelling (Table 1). Due to the high contact resistance it was only possible to transmit between 2 and 20 mA. There was a delay on 500 ms between each measurement and the integration time was 600 ms. The minimum number of stacks was 2 and the maximum number was 4. The maximum variation coefficient between the stacks was 1%.

The inversion program RES2DINV does not allow viewing and editing of the borehole resistivity data before inversion. Therefore the format of the borehole data files was modified to make it possible to plot data (Fig. 9) in pseudosections in the data visualization software Erigraph and to edit data in RES2DINV. Erigraph can e.g. plot pseudosections from Lund Imaging System and is distributed by ABEM Instrument AB. By plotting the data as a pseudosection an overview of the overall data quality is given before editing in RES2DINV, which can facilitate the omission of outliers from the measured data.

5. Results and discussion of measurements in horizontal boreholes

The prototype of the stiff electrode cables was effective and easy to use in practice, but problems still occurred during the measurements. One cable got stuck in a borehole and had to be left in the hole during the first stages of developing the prototype. This stimulated the development of a cable without any protuberances. Still it does not completely prevent the problem from recurring. Another problem was that a borehole collapsed before the measurements were done. As a consequence measurements were performed in holes of different length which gives an asymmetrical result. In this particular case the boreholes were re-drilled and the measurements could be performed in holes of equal length. However, it is too expensive and time consuming to re-drill the holes when the measurements are being used for regular production purposes.

The inversion of the borehole data gave a residual of 5.8% for the cross-hole dipole–dipole and 14.7% for the gradient array. The inversion of the combined data set gave also a residual of 14.7%.

Fig. 10 shows the inversion results of the resistivity measurements with the different array types and the combined data. The grey circles mark the positions of the electrodes in the two boreholes. The innermost electrode in both boreholes is positioned at 1 m and the tunnel wall is at 28.5 m. The results are viewed from above with the

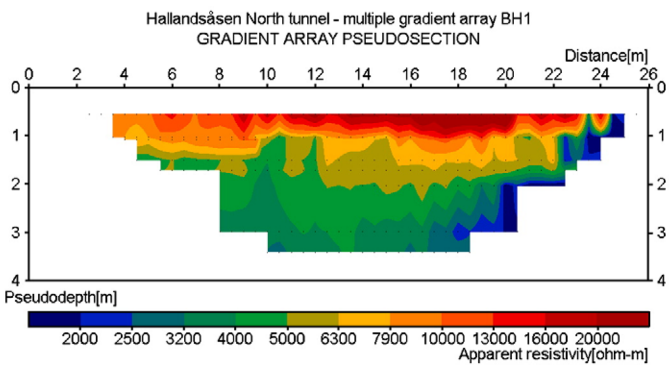

Fig. 9. An example on measured data plotted as a pseudosection. The example is the gradient data measured in one borehole plotted in Erigraph.

Author's personal copy

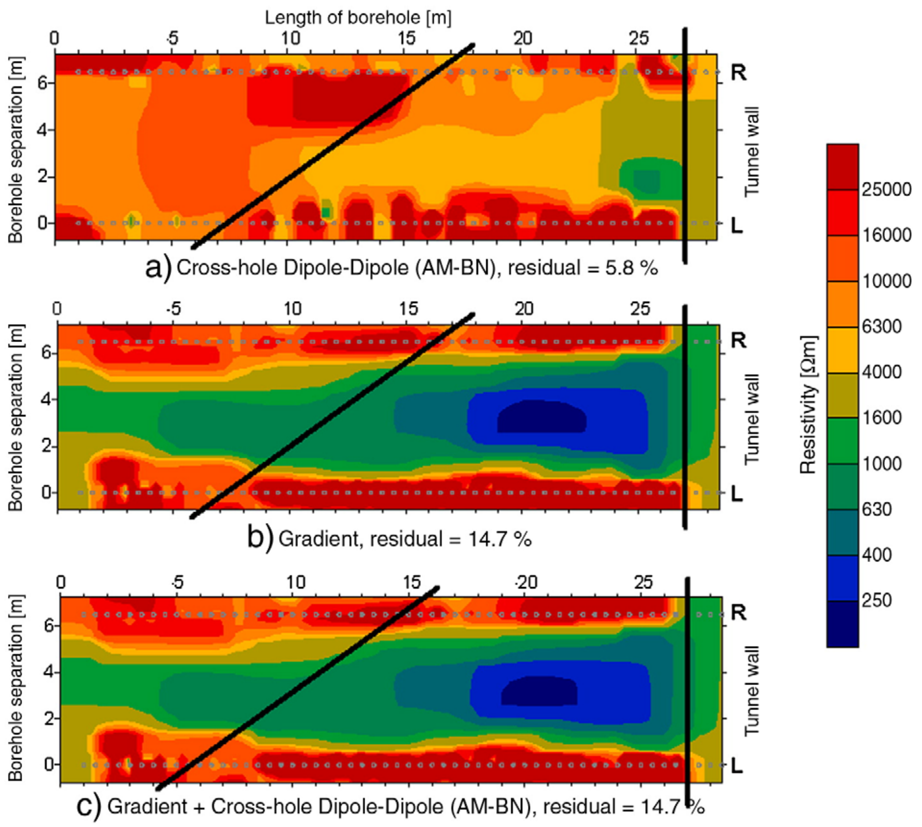

Fig. 10. The inversion results from the resistivity measurements using different electrode arrays. The boreholes are seen from above with the tunnel wall to the right in the figure. The left borehole, seen from the tunnel, is marked with *L* and the right borehole with *R*. The lines show probable structures. a) Cross-hole dipole–dipole array, b) Gradient array, c) Combination of gradient and cross-hole dipole–dipole. Grey circles mark the position of the electrodes. The electrode separation is 0.5 m.

tunnel wall to the right in the figures. The left borehole, seen from the tunnel, is marked with *L* whereas the right borehole is marked with *R*.

For all three results the resistivity close to the borehole is higher than 16,000 Ω m. The inversion result of the combined data set looks very much like the result using the gradient array. This is also confirmed by the absolute error value. Why the gradient array is so dominant has to be investigated in future work. Even though the results have a large difference in the resistivity of the area between the boreholes there is still a trend in the resistivity images. The line from 5 m in the left borehole to 17 m in the right borehole marks a transition from high resistivity to a slightly lower resistivity. Close to the tunnel wall the resistivity is low in all three examples.

As reference data for the interpretation of the resistivity data the information from a horizontal core drilling, called NA01, is used. NA01 is drilled perpendicular to the two boreholes and thereby parallel to the tunnel wall and therefore the information cannot be applied directly. The drilling report (left out here) showed that where it crosses the two test boreholes the lithology is gneiss. The geological structures here intersect the tunnel at an angle of 65–70°. This information together with the data from NA01 gives a rough estimated position of fractures and formation changes in the test boreholes, see Fig. 11.

By comparing the result from Fig. 10 with the estimated position of the structures found in NA01, it is clear that no fractures are resolved by the resistivity method. The fractures are presumably present but are not visible in the data. The fractures might be too narrow to be resolved with this electrode spacing and borehole separation. The data are most likely also influenced by 3D effects.

The transition from high resistivity to lower resistivity is probably a change in lithology from gneiss-granite to gneiss. The mineral

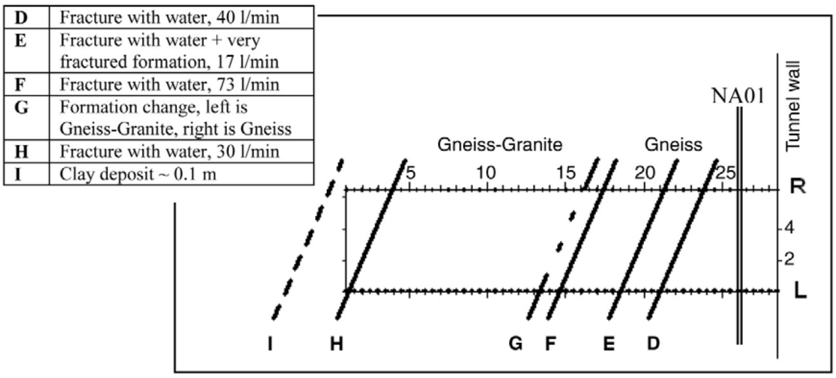

Fig. 11. The estimated projected position of the structures found in NA01. The nature of these fractures is seen in the table at the left. The approximated position of NA01 is shown with two parallel lines 3 m from the tunnel wall.

Author's personal copy

composition of the rock mass is different and probably most important is that the gneiss-granite contains less fractures than the gneiss (Wikman and Bergström, 1987). This would explain why the gneiss-granite has a higher resistivity than the gneiss. The low resistivity zone close to the tunnel wall is most likely caused by the shotcrete at the tunnel wall, which contains metal fibre reinforcements. In addition there might be rock reinforcements, e.g. rock bolts, which could affect the result. In an actual production phase shotcrete and rock reinforcement will not influence the measurements when performed in the tunnel front because they will not yet have been applied.

The numerical modelling showed that the water in the boreholes should not influence the resolution of the different arrays. The very high resistivity at the boreholes suggests that the measurements not are influenced by the water in the boreholes.

The residual for the measurements proved to be acceptable for the cross-hole dipole–dipole whereas for the gradient array it is rather high, but still acceptable. The high error could be expected because of the high resistive environment, limiting the transmitted current.

6. Conclusions

Probe holes are drilled up to 40 m ahead of a TBM in order investigate the rock conditions and the amount of water. If the geology is highly variable, representative information might not be obtained by drilling two or three probe holes because the area between the probes might be quite different. By performing small scale resistivity tomography between the boreholes a better image of the geological setting would be obtained and the operator would be better prepared of the upcoming 40 m ahead. The additional information might contribute to a more effective TBM advance. A development of an ERT system for horizontal boreholes is therefore important.

The numerical modelling showed that the best resolution of the inclined fracture zone was obtained using the multiple gradient array and a combination of AM-BN and multiple gradient. In addition the AM-BN proved to be the most insensitive towards non-parallel boreholes. The sensitivity pattern made it clear that the AM-BN has the largest sensitivity between the boreholes, while the gradient has the largest sensitivity close to the electrodes. The gradient array did also have the highest signal to noise ratio. This result can be used in the optimization of the protocols. The main conclusion was that AM-BN and multiple gradient array are the best for the actual measurements. The numerical modelling also showed that the water filled boreholes should not influence the results much.

The measurements in test boreholes showed that it most likely is possible to resolve the change from gneiss to gneiss-granite. The resistivity is low close to the tunnel wall because of the shotcrete. The very high resistivity at the boreholes proved that the low resistivity water in the boreholes did not have any visible effect on the result.

An important outcome of this study was that the prototype of the semi-rigid cable proved to work well. For production measurements it is suggested that electrode cables with an integrated glass fibre rod would work well. Measuring of reciprocal data for data quality assessment is suggested at least in a test and development phase. For a better data evaluation it would be worthwhile to obtain accurate reference data by making measurements in core drilled boreholes so that the resistivity results can be compared to the borehole logs. A further optimization of the protocol files is also vital, and in particular a study of the different 2D sensitivity patterns is considered to be essential. It would be interesting to do the measurements between more than one borehole in order to reduce the distance between the holes. In this case 3D inversion would be useful.

Acknowledgements

The work behind this paper was funded by SBUF (Development Fund of the Swedish Construction Industry), Banverket (Swedish Rail Administration) and Skanska-Vinci HB (SBUF project 11601), which is gratefully acknowledged. Drilling of test boreholes and invaluable logistic support during the field tests were provided by Skanska-Vinci HB. Our gratitude also goes to M.H. Loke for modifications made in Res2DMOD which made it possible to work with non-parallel boreholes. The comments and suggestions from two anonymous reviewers have significantly improved the quality of the paper.

References

Bing, Z., Greenhalgh, S.A., 2000. Cross-hole resistivity tomography using different electrode configurations. Geophysical Prospecting 48, 887–912.

Claerbout, J.F., Muir, F., 1973. Robust modelling with erratic data. Geophysics 38, 826–844.

Dahlin, T., Loke, M.H., 1998. Resolution of 2D Wenner resistivity imaging as assessed by numerical modelling. Journal of Applied Geophysics 38, 237–249.

Dahlin, T., Zhou, B., 2004. A numerical comparison of 2D resistivity imaging with 10 electrode arrays. Geophysical Prospecting 52, 379–398.

Dahlin, T., Bjelm, L., Svensson, C., 1999. Use of electrical imaging in site investigations for a railway tunnel through the Hallandsås Horst, Sweden. Quarterly Journal of Engineering Geology 32, 163–172.

Daily, W., Owen, E., 1991. Cross-borehole resistivity tomography. Geophysics 56 (8), 1228–1235.

Daily, W., Ramirez, A., LaBrecque, D., Barber, W., 1995. Electrical resistance tomography experiments at the Oregon Graduate Institute. Journal of Applied Geophysics 33 (4), 227–237.

Danielsen, B.E., Dahlin, T., Danielsen, J.E., 2005. Model study of the resolution of resistivity tomography with different electrode arrays. 11th European Meeting of Environmental and Engineering Geophysics.

Deceuster, J., Delgranche, J., Kaufmann, O., 2006. 2D cross-borehole resistivity tomographies below foundations as a tool to design proper remedial actions in covered karst. Journal of Applied Geophysics 60 (1), 68–86.

Denis, A., Marache, A., Obellianne, T., Breysse, D., 2002. Electrical resistivity borehole measurements: application to an urban tunnel site. Journal of Applied Geophysics 50 (3), 319–331.

French, H.K., Hardbattle, C., Binley, A., Winship, P., Jakobsen, L., 2002. Monitoring snowmelt induced unsaturated flow and transport using electrical resistivity tomography. Journal of Hydrology 267, 273–284.

Goes, B.J.M., Meekes, J.A.C., 2004. An effective electrode configuration for the detection of DNAPLs with electrical resistivity tomography. Journal of Environmental & Engineering Geophysics 9 (3), 127–142.

Guérin, R., 2005. Borehole and surface-based hydrogeophysics. Hydrogeology Journal 13 (1), 251–262.

LaBrecque, D.J., Ramirez, A.L., Daily, W.D., Binley, A.M., Schima, S.A., 1996. ERT monitoring of environmental remediation processes. Measurement Science and Technology 7 (3), 375–383.

Loke, M.H., 2001. RES3DMOD ver. 2.1 M.H.Loke on www.geoelectrical.com.

Loke, M.H., 2002. RES2DMOD ver. 3.01 M.H.Loke on www.geoelectrical.com.

Loke, M.H., 2004a. RES2DINV ver. 3.54 M.H.Loke on www.geoelectrical.com.

Loke, M.H., 2004b. Tutorial: 2-D and 3-D electrical imaging surveys: M.H.Loke on www.geoelectrical.com.

Loke, M.H., Acworth, I., Dahlin, T., 2003. A comparison of smooth and blocky inversion methods in 2D electrical imaging surveys. Exploration Geophysics 34, 182–187.

Parasnis, D.S., 1986. Principles of Applied Geophysics. Chapman and Hall.

Reynolds, J.M., 1997. An Introduction to Applied and Environmental Geophysics. John Wiley & Sons.

Rønning, J.S., 2003. Miljø- og samfunnstjenlige tunneler. Sluttrapport delprosjekt A, Forundersøkelser NGU. Report nr. 2003.077. (In Norwegian).

Tsourlos, P., Ogilvy, R., Williams, G., 2003. Time-lapse monitoring in si.ngle boreholes using electrical resistivity tomography. Journal of Environmental and Engineering Geophysics 8, 1–14.

Wikman, H., Bergström, J., 1987. Beskrivning till Berggrundskartan Halmstad SV Swedish Geological Survey, Uppsala. (In Swedish).

Wilkinson, P.B., Chambers, J.E., Lelliott, M., Wealthall, G.P., Ogilvy, R.D., 2008. Extreme sensitivity of crosshole electrical resistivity tomography measurements to geometric errors. Geophysical Journal International 173, 49–62.